Received January 2000
Revised August 2000
Accepted August 2000

Thermal-fluid transport phenomena in strongly heated channel flows

Shuichi Torii
Department of Mechanical Engineering, Kagoshima University, Kagoshima, Japan, and
Wen-Jei Yang
Mechanical Engineering and Applied Mechanics, University of Michigan, Ann Arbor, Michigan, USA

Keywords *Turbulent kinetic theory, Laminar flow, Channels, Transport*

Abstract *A theoretical study is performed to investigate transport phenomena in channel flows under uniform heating from either both side walls or a single side. The anisotropic $\bar{t^2} - \varepsilon_t$ heat-transfer model is employed to determine thermal eddy diffusivity. The governing boundary-layer equations are discretized by means of a control volume finite-difference technique and numerically solved using a marching procedure. It is found that under strong heating from both walls, laminarization occurs as in the circular tube flow case; during the laminarization process, both the velocity and temperature gradients in the vicinity of the heated walls decrease along the flow, resulting in a substantial attenuation in both the turbulent kinetic energy and the temperature variance over the entire channel cross section; both decrease causes a deterioration in heat transfer performance; and in contrast, laminarization is suppressed in the presence of one-side-heating, because turbulent kinetic energy is produced in the vicinity of the other insulated wall.*

Nomenclature

c_p = specific heat at constant pressure, J/(kgK)
$C_\mu, C_1, C_3, C_{\mu 1}, C_{\varepsilon 2}$ = turbulence model constants for velocity field
$C_\lambda, C_{p1}, C_{p2}, C_{p3}$ = turbulence model constants for temperature field
$C_s, C_{st}, C_{d1}, C_{d2}$ = turbulence model constants for temperature field
$f_\mu, f_{\varepsilon 1}, f_{\varepsilon 2}$ = turbulence model functions for velocity field
$f_\lambda, f_{p1}, f_{p2}, f_{p3}, f_{d1}, f_{d2}$ = turbulence model functions for temperature field
g = acceleration of gravity, m/s^2
G = mass flux of gas flow, $kg/(m^2s)$
Gr = Grashof number, $gqwH^4/(v^2\lambda T)$ in
h = heat transfer coefficient, W/m^2K
H = channel height, m
k = turbulent kinetic energy, m^2/s^2
M = the number of mesh
Nu = Nusselt number, $2Hh/\lambda$
P = time-averaged pressure, Pa
Pr = Prandtl number
Pr_t = turbulent Prandtl number
q = heat flux, W/m^2
q^+w = dimensionless heat flux parameter, equation (14)
Re = Reynolds number, $2u_mH/v$
R_t = turbulent Reynolds number, $k^2/(\varepsilon v)$
$R\tau$ = dimensionless distance, y^+
St = Stanton number, $qw/(\rho c_p u_m (Tw–Tb))$
T^+ = dimensionless time-averaged temperature, $(T_w–T)/(qw/\rho c_p u^*)$
T = time-averaged temperature, K
t = fluctuating temperature component, K
t^* = friction temperature, $qw/(\rho c_p u^*)$, K
$\bar{t^2}$ = temperature variance, K^2

International Journal of Numerical Methods for Heat & Fluid Flow, Vol. 10 No. 8, 2000, pp. 802-823.

U, V = time-averaged velocity components in axial, and normal-wall directions respectively, m/s

U_i, u_i = time-averaged and fluctuating velocity components in the x_i directions respectively, m/s

u_m = mean velocity over channel cross section

u, v, w = fluctuating velocity components in axial, wall-normal and tangential directions respectively, m/s

u^* = friction velocity, m/s

u^+ = dimensionless velocity, U/u*

x_i = coordinates, m

y = wall-normal coordinate, m

y^+ = dimensionless distance, $u^* \delta / v$

Greek letters

α = thermal diffusivity, m^2/s

α_2, α_2 = turbulence model constants for temperature field

ρ = density, kg/m^3

ε = distance from wall, m

δ = turbulent energy dissipation rate, m^2/s^3 $\varepsilon = \nu \overline{\frac{\partial u_i}{\partial x_j}} \overline{\frac{\partial u_i}{\partial x_j}}$

ε_t = dissipation rate of temperature variance, K^2/s $\varepsilon_t = \alpha \overline{\frac{\partial t}{\partial x_i}} \overline{\frac{\partial t}{\partial x_i}}$

λ, λ_t = molecular and turbulent thermal conductivities respectively, W/(Km)

μ, μ_t = molecular and turbulent viscosities respectively, Pa sec

v = fluid kinematic viscosity, m^2/s

$\sigma_k, \sigma_\varepsilon$, = turbulence model constants for diffusion of k, ε respectively

θ^+ = dimensionless temperature, $\theta^+ = \frac{T - T_c}{T_w - T_c}$

Subscripts

b = bulk

c = center or insulated wall

in = inlet

max = maximum

w = wall

Superscripts

– = time-averaged value

Introduction

When a gas in a tube is heated with extremely high heat flux, the flow may be laminarized; that is, a transition from turbulent to laminar flows occurs at a higher Reynolds number than the usual critical value, i.e. Re = 2,300. This phenomenon is referred to as laminarization. Both the criteria for its occurrence and its heat transfer characteristics have been reported by several investigators (Bankston, 1970; Coon and Perkins, 1970; McEligot *et al.*, 1970; Perkins *et al.*, 1973; Mori and Watanabe, 1979; Ogawa *et al.*, 1982). Kawamura (1979) and Torii *et al.* (1990) analyzed laminarization phenomena by means of *k-kL* and *k-ε* models respectively. Ogawa and Kawamura (1986; 1987) measured the local friction factor and local Stanton number in the laminarizing flow and predicted their substantial attenuation during laminarization using the *k-kL* model modified by Kawamura (1979). Furthermore, Torii *et al.* (1993) and Torii and Yang (1997) investigated the flow and thermal fields in a strongly heated circular tube by means of a Reynolds stress turbulence model and a two-equation heat transfer model respectively. They reported that:

(1) even with a substantial reduction in heat transfer, i.e. when laminarization takes place, the turbulent kinetic energy does not disappear completely; and

(2) laminarization due to strong heating causes both a reduction in the Reynolds stress and an amplification of the inherent anisotropy of the turbulence structure;

(3) both the temperature variance and the turbulent heat flux are also diminished over the whole tube cross section in the flow direction; and

(4) although both the velocity dissipation time scale and the temperature dissipation time scale are substantially amplified in the laminarizing flow, their ratio is only slightly increased.

Recently, Ezato *et al.* (1999) predicted a strongly heated forced gas flows at low Reynolds numbers in the vertical circular tubes using the k-ε turbulence model of Abe *et al.* (1994), in which the calculation was compared with the experimental results measured by Shehata (1984).

It is very important to investigate how passage geometry affects the laminarizing gas flow under strong heating. Torii *et al.* (1991) studied heat and fluid flow transport phenomena in concentric annuli under high heat flux heating. They disclosed that:

(1) when the gas flow is strongly heated with the same heat flux level from inner and outer tube walls, the local heat transfer coefficients on both walls approach the laminar values along the flow, that is, the laminarization takes place;

(2) the existing criteria of laminarization for circular tube flows can be applied to annular flows as well if the occurrence of laminarization is estimated using a dimensionless heat flux parameter $q^{+}w$; but

(3) annular flows heated strongly from only one side are less vulnerable to laminarization even if the usual criteria are satisfied.

A similar numerical study has been reported by Fujii *et al.* (1991), who employ three difference turbulence models, i.e. k-ε, $k-\varepsilon-\overline{uv}$, and $k-kL-\overline{uv}$. The occurrence of laminarization is clearly affected by the passage geometry and may be also affected by the boundary condition of the heat source. Thus, the effects of passage geometry and boundary condition on the occurrence of laminarization warrant further investigation.

The purpose of the present study is to investigate heat transport phenomena in channel flows under two conditions:

(1) where both walls are simultaneously heated with uniform heat flux; and

(2) where only one-side wall is heated.

The anisotropic $\bar{t^2}-\varepsilon_t$ heat transfer model of Torii and Yang (1996) and the anisotropic k-ε turbulence model of Myong and Kasagi (1990) are employed to determine the mechanism of heat transport phenomena. The turbulent thermal conductivity λ_t is determined using the temperature variance, $\bar{t^2}$, and the dissipation rate of temperature fluctuations, ε_t, together with k and ε. Emphasis is placed on the effects of the boundary condition on the laminarizing flow, based on the numerical results, i.e. the turbulent kinetic energy, temperature variance, velocity, and temperature profiles.

Governing equations and numerical scheme

Consideration is given to a steady turbulent flow in a strongly heated channel. The physical configuration and the coordinate system are shown in Figure 1. In this analysis, the dependence of gas properties on temperature, as well as changes in gas density, must be taken into account (Schlighting, 1968). The continuity, momentum and energy equations for an incompressible fluid, disregarding buoyancy force, read:

Continuity equation:

$$\frac{\partial \overline{\rho}\, U_i}{\partial x_i} = 0 \tag{1}$$

Momentum equation:

$$\overline{\rho} U_j \frac{\partial U_i}{\partial x_j} = -\frac{\partial P}{\partial x_i} + \frac{\partial}{\partial x_j}\left(\mu \frac{\partial U_i}{\partial x_j} - \overline{\rho u_i u_j}\right) \tag{2}$$

Energy equation:

$$c_p \overline{\rho} U_i \frac{\partial T}{\partial x_i} = \frac{\partial}{\partial x_i}\left(\lambda \frac{\partial T}{\partial x_i} - c_p \overline{\rho u_i t}\right) \tag{3}$$

Here, the turbulent fluctuations of λ, μ and c_p through temperature fluctuation have been discounted. The term for body force in the momentum equation is also negligible, because a small diameter tube was employed and throughout the calculation, the buoyancy parameter Gr/Re_{in}^{2} was less than 0.1 so that forced convection may be expected to dominate.

In order to solve numerically the turbulent heat transport problems, the turbulent heat flux in the energy equation, as a simple method, is modeled by using the classical Boussinesq approximation. That is, the unknown turbulent thermal conductivity λ_t is obtained from the definition of the specific heat c_p, the turbulent viscosity μ_t and the turbulent Prandtl number Pr_t as $\lambda_t = c_p \mu_t / Pr_t$. However, the numerical calculation with this formulation gives no more detailed information on heat transport phenomena, such as temperature fluctuations and turbulent heat flux. To achieve this objective, the one- and two-equation models for thermal field and the turbulent heat flux equation model are employed. Recently, McEligot *et al.* (1998) carried out an assessment of several turbulence models in internal gas

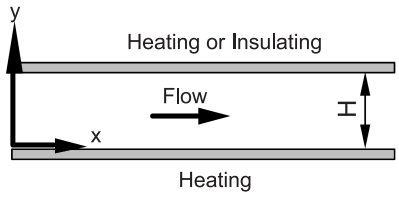

Figure 1.
A schematic of the physical system and coordinates

flows under strong heating. They reported that a turbulence model capable of reproducing the correct near-wall limiting behavior of turbulent quantities is recommended to calculate strongly heated turbulent or laminarizing gas flows. In the present study, the $\overline{t^2} - \varepsilon_t$ model for thermal field is applied to analyze gas flows in a strongly heated channel flows, because the model introduced in the following satisfies the requirement of near-wall limiting behavior. The turbulent heat flux $-c_p\bar{\rho}\,\overline{u_i t}$ in equation (3) can be given in the form of an anisotropic eddy-diffusivity representation (Torii and Yang, 1996), as:

$$\begin{aligned} -c_p\overline{\rho}\overline{u_i t} &= C_\lambda f_\lambda c_p \overline{\rho} k \left(\frac{k}{\varepsilon}\right)^{-1} \left(\frac{\overline{t^2}}{\varepsilon_t}\right)^{2} \frac{\partial T}{\partial x_i} \\ &- f_\lambda c_p \overline{\rho} k \left(\frac{k}{\varepsilon}\right)^{-2} \left(\frac{\overline{t^2}}{\varepsilon_t}\right)^{4} \left\{ \alpha_1 \left(\frac{\partial U_i}{\partial x_j} + \frac{\partial U_j}{\partial x_i}\right) + \alpha_2 \left(\frac{\partial U_i}{\partial x_j} - \frac{\partial U_j}{\partial x_i}\right) \right\} \frac{\partial T}{\partial x_j}, \end{aligned} \tag{4}$$

where $C\lambda$ is a model constant and $f\lambda$ is a model function. In the present study, a two-equation model for heat transport capable of predicting the anisotropic turbulent heat fluxes (Torii and Yang, 1996) is used to obtain $\overline{t^2}$ and ε_t in equation (4). The transport equations for $\overline{t^2}$ and ε_t are expressed in tensor form as:

$$c_p\overline{\rho}U_j \frac{\partial \overline{t^2}}{\partial x_j} = \frac{\partial}{\partial x_j}\left(\lambda \frac{\partial \overline{t^2}}{\partial x_j} + C_s \frac{k}{\varepsilon} c_p \overline{\rho u_i u_j} \frac{\partial \overline{t^2}}{\partial x_i}\right) - 2c_p\overline{\rho}\overline{u_j t}\frac{\partial T}{\partial x_j} - 2c_p\overline{\rho}\varepsilon_t \tag{5}$$

and

$$\begin{aligned} c_p\overline{\rho}U_j \frac{\partial \varepsilon_t}{\partial x_j} &= \frac{\partial}{\partial x_j}\left(\lambda \frac{\partial \varepsilon_t}{\partial x_j} + C_{st} \frac{k}{\varepsilon} c_p \overline{\rho u_i u_j} \frac{\partial \varepsilon_t}{\partial x_i}\right) \\ &- C_{p1} f_{p1} c_p \overline{\rho} \frac{\varepsilon_t}{\overline{t^2}} \overline{u_j t} \frac{\partial T}{\partial x_j} - C_{p2} f_{p2} c_p \overline{\rho} \frac{\varepsilon}{k} \overline{u_j t} \frac{\partial T}{\partial x_j} - C_{p3} f_{p3} c_p \overline{\rho} \frac{\varepsilon_t}{k} \overline{u_i u_j} \frac{\partial U_i}{\partial x_j} \\ &- C_{d1} f_{d1} c_p \overline{\rho} \frac{\varepsilon_t{}^2}{\overline{t^2}} - C_{d2} f_{d2} c_p \overline{\rho} \frac{\varepsilon\,\varepsilon_t}{k} \end{aligned} \tag{6}$$

respectively. Notice that the model satisfies the requirement of near-wall limiting behavior in channel flows (Torii and Yang, 1996). The empirical constants and model functions in equations (4), (5) and (6) are summarized in Table I.

In general, the Reynolds stress turbulence model is employed to obtain the Reynolds stress $-\overline{\rho u_i u_j}$ in equations (2), (5) and (6). In the present study, these stresses are determined based on the anisotropic eddy diffusivity representation (Myong and Kasagi, 1990), because much shorter computing time is achieved than the utilization of the Reynolds stress model. Its presentation is as follows:

$$-\overline{\rho u_i u_j} = -\frac{2}{3}\delta_{ij}\overline{\rho}k - \mu_t\left(\frac{\partial U_i}{\partial x_j}+\frac{\partial U_j}{\partial x_i}\right)+\frac{k}{\varepsilon}\mu_t\sum_{\beta=1}^{3} C_\beta\left(S_{\beta ij}-\frac{1}{3}S_{\beta pp}\delta_{ij}\right)$$
$$+\frac{2}{3}\mu_t\frac{k}{\varepsilon}(-\delta_{ij}-\delta_{in}\delta_{jn}+4\delta_{im}\delta_{jm})\left(\frac{\partial\sqrt{k}}{\partial x_n}\right)^2 \quad (7)$$

where

$$S_{1ij} = \frac{\partial U_i}{\partial x_\gamma}\frac{\partial U_j}{\partial x_\gamma}$$
$$S_{2ij} = \frac{1}{2}\left(\frac{\partial U_\gamma}{\partial x_i}\frac{\partial U_j}{\partial x_\gamma}+\frac{\partial U_\gamma}{\partial x_j}\frac{\partial U_i}{\partial x_\gamma}\right)$$
$$S_{3ij} = \frac{\partial U_\gamma}{\partial x_i}\frac{\partial U_\gamma}{\partial x_j}$$

Here, the turbulent viscosity μ_t can be expressed in terms of the turbulent kinetic energy k and its dissipation rate ε, referring to the Kolmogorov-Prandtl's relation (Rodi, 1982), as

$$\mu_t = C_\mu f_\mu \bar{\rho}\frac{k^2}{\varepsilon}\ . \quad (8)$$

C_μ and f_μ are a model constant and a model function respectively. Both transport equations developed by Myong and Kasagi (1990) read

$$\bar{\rho}U_j\frac{\partial k}{\partial x_j} = \frac{\partial}{\partial x_j}\left\{\left(\mu+\frac{\mu_t}{\sigma_k}\right)\frac{\partial k}{\partial x_j}\right\} - \bar{\rho}\,\overline{u_i u_j}\frac{\partial U_i}{\partial x_j} - \bar{\rho}\varepsilon \quad (9)$$

$$\bar{\rho}U_j\frac{\partial \varepsilon}{\partial x_j} = \frac{\partial}{\partial x_j}\left\{\left(\mu+\frac{\mu_t}{\sigma_\varepsilon}\right)\frac{\partial \varepsilon}{\partial x_j}\right\} - C_{\varepsilon 1}f_{\varepsilon 1}\bar{\rho}\frac{\varepsilon}{k}\overline{u_i u_j}\frac{\partial U_i}{\partial x_j} - C_{\varepsilon 2}f_{\varepsilon 2}\bar{\rho}\frac{\varepsilon^2}{k} \quad (10)$$

C_{P1}	1.20	C_{P2}	0.51	C_{P3}	0.52	C_s	0.11
f_{P1}	1.0	f_{P2}	1.0	f_{P3}	1.0	C_{st}	0.11
C_λ	0.078	B_λ	3.4	A_λ	35.6		
C_{d1}	2.0	C_{d2}	0.8	α_1	0.056	α_2	0.014
R_h	$(k/v)(k/\varepsilon)^{-1}(t^{-2}/\varepsilon_t)^2$						
f_{d1}	$1-\exp(-\sqrt{\frac{R_h}{10}})$						
f_{d2}	$\{1-\exp(-\frac{y^+}{8})\}^2$						
f_λ	$\{1-\exp(-\frac{y^+}{A_\lambda})\}^2(1+\frac{B_\lambda}{R_h^{3/4}})$						

Table I. Empirical constants and model functions in the anisotropic $t^2-\varepsilon_t$ heat transfer model

The empirical constants and model functions in equations (8), (9) and (10) are presented in Table II. A combination of the k-ε model for velocity field and the $\bar{t^2} - \varepsilon_t$ model for thermal field is applied to analyze gas flows in a strongly heated channel flows.

A set of governing equations are solved using the control volume finite-difference procedure developed by Patankar (1980). The power-law scheme for the convection-diffusion formulation is employed to link the convection-diffusion terms. Since all turbulent quantities as well as the time-averaged streamwise velocity vary rapidly in the near-wall region, the size of nonuniform cross-stream grids increases with a geometric ratio from the wall towards the center line. The maximum control volume size near the center line is always kept at less than 1 per cent of channel height. To ensure the accuracy of calculated results, at least two control volumes are located in the viscous sublayer. Throughout the numerical calculations, the number of control volumes is properly selected between 72 and 98 to obtain a grid-independent solution, resulting in no appreciable difference between the numerical results with different grid spacing, as shown. The discretized equations are solved from the inlet in the downstream direction by means of a marching procedure, since these equations are parabolic. The maximum step-size in the streamwise direction is limited to five times the minimum size in the wall-normal direction of the control volume. At each axial location, the thermal properties for control volumes are determined from the axial pressure and temperature using a numerical code of reference (Propath Group, 1987).

The hydrodynamically fully-developed isothermal flow is assumed at the starting point of the heating section. The following boundary conditions are used at the walls:

Case A (both-sides heating)

$y = 0$: $U = k = 0$,

$$\varepsilon = 2\,v\left(\frac{\partial\sqrt{k}}{\partial y}\right)^2, \frac{\partial \bar{t^2}}{\partial y} = 0, \varepsilon_t = \alpha\frac{\partial^2(\bar{t^2}/2)}{\partial y^2}, \text{ and}$$

$$-\frac{\partial T}{\partial y} = \frac{q_w}{\lambda_w}(\text{constant heat flux})$$

$y = H$: $U = k = 0$,

C_μ	σ_k	σ_ε	$C_{\varepsilon 1}$	$C_{\varepsilon 2}$	C_1	C_3	$f_{\varepsilon 1}$
0.09	1.4	1.3	1.4	1.8	0.8	–0.15	1.0
f_μ	$(1 + \frac{3.45}{\sqrt{R_t}})\{1 - \exp(-\frac{y^+}{70})\}$						
$f_{\varepsilon 2}$	$[1 - \frac{2}{9}\exp\{-(\frac{R_t}{6})^2\}]\{1 - \exp(-\frac{y^+}{5})\}^2$						

Table II.
Empirical constants and model functions in the anisotropic k-ε turbulence model

$$\varepsilon = 2\,v\Big(\frac{\partial\sqrt{\mathrm{k}}}{\partial \mathrm{y}}\Big)^2, \frac{\partial \mathrm{t}^{\bar{2}}}{\partial \mathrm{y}} = 0.\ \varepsilon_{\mathrm{t}} = \alpha\frac{\partial^2(\mathrm{t}^{\bar{2}}/2)}{\partial \mathrm{y}^2},\ \text{and}$$

$$\frac{\partial \mathrm{T}}{\partial \mathrm{y}} = \frac{\mathrm{q_w}}{\lambda_{\mathrm{w}}}\,(\text{constant heat flux})$$

Case B (one-side heating)

y = 0: U = k = 0,

$$\varepsilon = 2\,v\Big(\frac{\partial\sqrt{\mathrm{k}}}{\partial \mathrm{y}}\Big)^2, \frac{\partial \mathrm{t}^{\bar{2}}}{\partial \mathrm{y}} = 0.\ \varepsilon_{\mathrm{t}} = \alpha\frac{\partial^2(\mathrm{t}^{\bar{2}}/2)}{\partial \mathrm{y}^2},\ \text{and}$$

$$-\frac{\partial \mathrm{T}}{\partial \mathrm{y}} = \frac{\mathrm{q_w}}{\lambda_{\mathrm{w}}}\,(\text{constant heat flux})$$

y = H: U = k = 0,

$$\varepsilon = 2\,v\Big(\frac{\partial\sqrt{\mathrm{k}}}{\partial \mathrm{y}}\Big)^2, \frac{\partial \mathrm{t}^{\bar{2}}}{\partial \mathrm{y}} = 0.\ \varepsilon_{\mathrm{t}} = \alpha\frac{\partial^2(\mathrm{t}^{\bar{2}}/2)}{\partial \mathrm{y}^2},\ \text{and}\ \frac{\partial \mathrm{T}}{\partial \mathrm{y}} = 0\ (\text{insulation})$$

Based on the above boundary conditions, the computations are processed in the following order:

(1) The initial values of U, k, ε, T, $\mathrm{t}^{\bar{2}}$ and ε_t are specified and assigned a constant axial pressure gradient. Here, the values of U, k and ε in the hydrodynamically fully-developed isothermal channel flow are employed as the initial values.

(2) The equations of U, k, ε, T, $\mathrm{t}^{\bar{2}}$ and ε_{t} are solved using the boundary conditions given here.

(3) Step 2 is repeated until the criterion of convergence is satisfied. It is set at

$$\max\Big|\frac{\phi^{\mathrm{M}} - \phi^{\mathrm{M-1}}}{\phi^{\mathrm{M-1}}_{\max}}\Big| < 10^{-4} \tag{11}$$

for all variables ϕ (U, k, ε, T, t^{-2} and ε_{t}). The superscripts M and M–1 in equation (11) indicate two successive iterations, while the subscript "max" refers to a maximum value over the entire field of iterations.

(4) New values of U, k, ε, T, $\mathrm{t}^{\bar{2}}$ and ε_{t} are calculated by correcting the axial pressure gradient.

(5) Steps 2-4 are repeated until the conservation of the streamwise flow rate is satisfied under the criterion

$$\left|\frac{\int U_{cp}dy - \int U_{in}dy}{\int U_{in}dy}\right| \leq 10^{-5} \tag{12}$$

and the convergent values of U, k, ε, T, $\bar{t^2}$ and ε_t are evaluated. Here, U_{cp} is the axial velocity under the correction process and U_{in} is that at the inlet of the channel.

(6) Steps 2-5 are repeated until x reaches the desired length from the inlet.

In the present study, the nondimensional heat flux parameter q^+w is employed to indicate the magnitude of heat flux at the channel wall. This parameter, originally proposed by Nemira *et al.* (1980) for determining thermal transport phenomena in concentric annular gas flows, is defined as

$$q_w^+ = \frac{d_{in}q_{in} + d_{out}q_{out}}{d_{in} + d_{out}} \frac{1}{(Gc_pT)_{in}} \quad , \tag{13}$$

where d_{in} and d_{out} are, respectively, the inner and outer tube diameters of the annulus, and q_{in} and q_{out} correspond to heat fluxes on the inner and outer walls of the annulus. The above parameter was also used for determining laminarization phenomena in concentric annuli heated with high heat flux (Torii *et al.*, 1991). When applying equation (13) to two-dimensional channel, it is reduced for Cases A and B, as

$$q_w^+ = \frac{q_w}{(Gc_pT)_{in}} \tag{14a}$$

and

$$q_w^+ = \frac{1}{2}\frac{q_w}{(Gc_pT)_{in}} \tag{14b}$$

respectively. Note that for the Case A, the parameter defined in equation (14a) is the same as that employed for the laminarizing gas flow in the strongly heated circular tube. The ranges of the parameters are the nondimensional heat flux parameter $q^+w<0.009$; the inlet Reynolds number, i.e. the Reynolds number at the onset of heating Re_{in} = 8,500; and the inlet gas (nitrogen) temperature T_{in} = 273K. Numerical computations were performed on a personal computer (32 bit).

To verify the k-ε turbulence and two-equation heat-transfer models and to determine the reliability of the computer code, heat transfer coefficients and velocity, and temperature profiles are calculated. The model is applied to channel flow with a low uniform wall heat flux. The variation of the gas properties only slightly affects the velocity and thermal fields. The numerical result is obtained at a location of 150 times the hydraulic diameter downstream from the inlet where both thermally and hydrodynamically fully-developed conditions prevail.

Figure 2 illustrates the heat transfer coefficients at different mesh sizes in the form of Nusselt number Nu versus Reynolds number Re. Figures 2(a) and (b) correspond, respectively, to the numerical results for channel flows where both walls are heated simultaneously with uniform heat flux, and where one wall is heated and the other wall insulated. For comparison, theoretical solutions (Kays and Crawford, 1980) of laminar and turbulent heat transfer are superimposed in the figure in solid straight lines. One observes that the calculated Nusselt numbers, which are depicted with the solid symbols, are in excellent agreement with the correlation in the higher Reynolds number region,

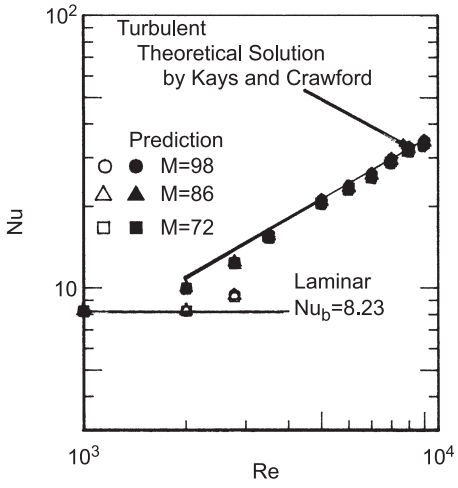

(a) two-sides heating

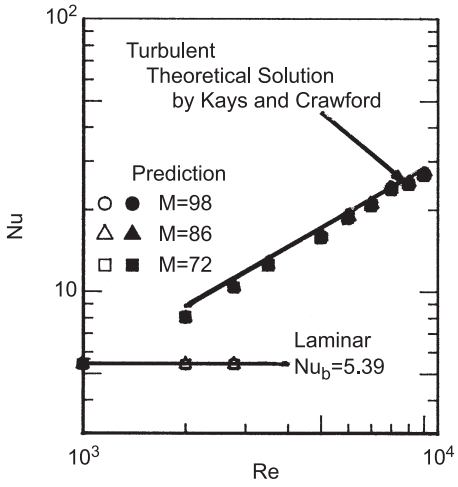

(b) one-side heating

Figure 2.
Predicted Nusselt numbers in the fully-developed channel flow

over 3,000. However, the original models employed here fail to reproduce the heat transfer behavior in the lower-Reynolds number region, i.e. in the transition region (Schlighting, 1968). That is, the transition from turbulent to laminar flow is predicted to occur at much lower than the transition Reynolds number and the transition itself is somewhat asymptotic rather than stepwise. It is apparent that the prediction efficiency in the turbulent-to-laminar transition region is of crucial importance in the examination of the laminarization phenomena.

An attempt is made to modification to take the slight shortcoming of turbulence models employed here into account. In the analysis on laminarization phenomena by means of the k-ε turbulence model, Torii *et al.* (1990) reported that the transition Reynolds number, from laminar to turbulent flows, is obtained by modifying the model constant, $C_{\varepsilon 1}$, and model function $f_{\varepsilon 1}$ in the ε equation. Based these consideration, $C_{\varepsilon 1}$ and $f_{\varepsilon 1}$ are determined by a trial-and-error process so as to simulate the heat transfer behavior in the transition region. In the present study, the value 1.39 for $C_{\varepsilon 1}$ and the following function of the turbulent Reynolds number for $f_{\varepsilon 1}$, are used.

$$f_{\varepsilon 1} = 1 + 0.25 \exp\left(\frac{-R_t}{25}\right) \tag{15}$$

Using a combination of the slightly modified k-ε turbulence model and the original two-equation heat transfer model, the predicted Nusselt numbers are superimposed in Figure 2(a) and (b) with open symbols. It is observed that:

(1) calculated values of the Nusselt number are in excellent agreement with correlations in the Reynolds number region over 3,000; and

(2) the turbulence model reproduces the heat transfer characteristics in the lower Reynolds number region; that is, the transition from turbulent to laminar flows is predicted to occur at about Re = 3,000.

In the following, the modified model was employed to predict the thermal transport phenomena in the strongly heated channel flows. It is observed, through the calculation, that there is only a slight change in the Nusselt number even if the number of control volumes is set between 72 and 98. Therefore, no appreciable difference appears between the numerical results with different grid spacing.

Figure 3 illustrates the calculated time-averaged velocity profiles (dimensionless velocity u^+ versus y^+) at Re = 1,000 and 10,000. The results are compared with the universal wall law. Here, numerical results are obtained for channel flows heated from both sides. The result at Re = 10,000 predicts a velocity profile with the well-known characteristics of the logarithmic region. The velocity profile at Re = 1,000 is in good agreement with the laminar one, i.e. $u^+=y^+$. The corresponding distributions of the time-averaged temperature in the thermal field are illustrated in Figure 4 in the form of T^+ versus y^+. The numerical result at Re = 10,000 is in accordance with the law of the wall for a

thermal boundary layer, and the laminar profile $T^+ = Pry^+$ is predicted at Re = 1,000. The above numerical results show that the validity of the computer code and the accuracy of the turbulence models employed here are borne out.

Results and discussion

Two sets of calculations to determine heat transport phenomena in channel flows with:

(1) both walls heated simultaneously with uniform heat flux; or

(2) one wall heated and the other wall insulated, are explained below.

Figure 5 illustrates the local heat-transfer coefficients in strongly heated channel flows in the form of Stanton number St_b versus Reynolds number Re_b, with q^+w as the parameter. Figures 5(a) and (b) correspond to the results for two-sides and one-side heating (Cases A and B) respectively. The inlet bulk Reynolds number is fixed at 8,500. Theoretical solutions for turbulent and laminar heat transfer in the thermally and hydrodynamically fully-developed channel flows (Kays and Crawford, 1980) are superimposed in the figure in a solid straight lines. In Figure 5, a reduction in the bulk Reynolds number signifies a change in the location along the channel, because the bulk Reynolds number decreases from the inlet with the axial distance resulting from an increase in the molecular viscosity by heating. The numerical results for Cases A and B show that the local Stanton numbers at $q^+w = 0.0025$ first decrease in the thermal entrance region, then increase, approaching the turbulent correlation further downstream. This suggests that no laminarization will occur. On the contrary, as the flow goes downstream, the predicted Stanton numbers at $q^+w = 0.0043$, whose level causes the laminarization in the strongly

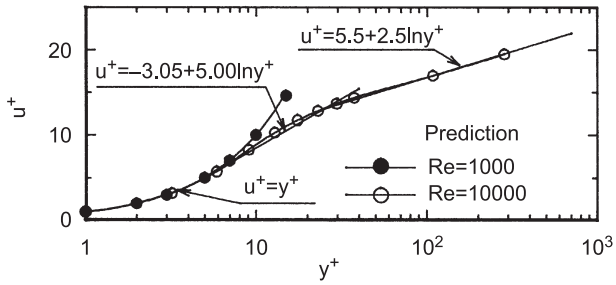

Figure 3.
Radial distributions of time-averaged velocity in the fully-developed channel flow for Re = 1,000 and 10,000

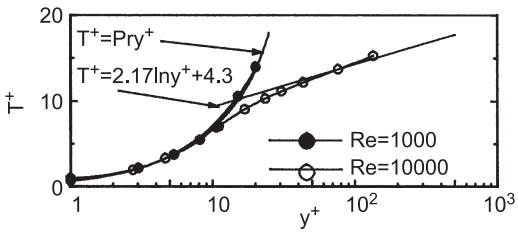

Figure 4.
Radial distributions of time-averaged temperature in the fully-developed channel flow for Re = 1,000 and 10,000

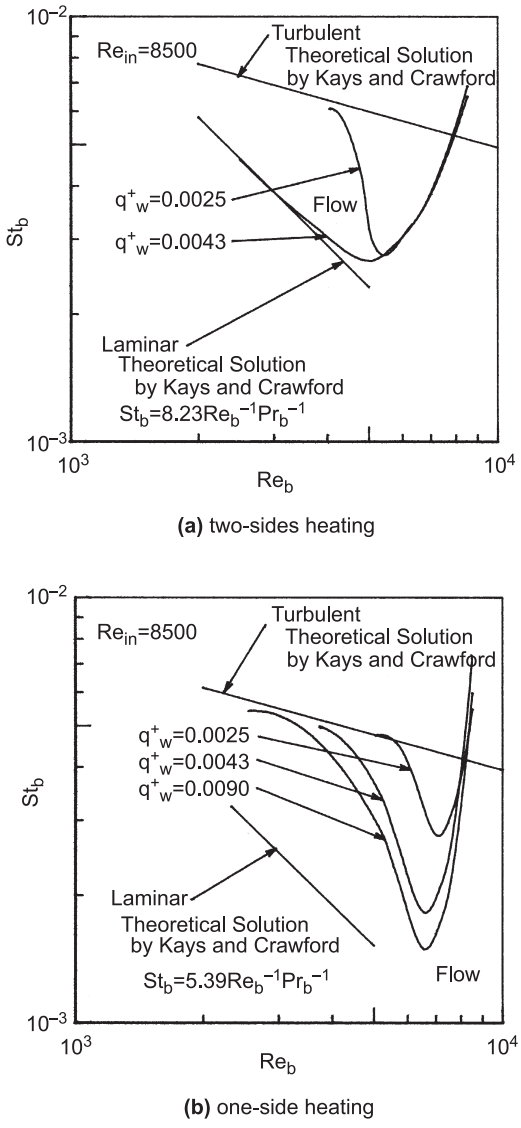

Figure 5.
Predicted local Stanton number with Reynolds number as a function of nondimensional heat flux parameters under different boundary conditions

heated circular tube, depart from the turbulent heat-transfer correlation and approach the laminar correlation, as shown in Figure 5(a). Bankston (1970) pointed out that the substantial reduction in St_b along the flow is due to the occurrence of laminarization. In other words, if the channel is strongly heated from both walls, the fluid flow is laminarized as in the circular tube flow case. However, in Figure 5(b) the local Stanton number at $q^+w = 0.0043$ decreases in the thermal entrance region, then recovers along the flow and eventually approaches the turbulent correlation equation further downstream. This transport phenomenon provides a striking contrast to that for Case A at the

corresponding dimensionless heat flux. When heat flux on a single heating wall becomes higher, the predicted local Stanton number, as seen in Figure 5(b), approaches the turbulent correlation downstream, even at $q^+w = 0.0090$, i.e. a level that under two-sided heating completely laminarizes the tube flow. In other words, if a channel is heated exclusively from only one wall, the fluid flow can not be laminarized and is a striking contrast to the tube flow case. This behavior in the channel flow is the same as the thermal-fluid transport characteristics in the annuli heated strongly from only one side, as mentioned in the introduction. The occurrence of laminarization is thus clearly affected by boundary conditions.

An attempt is made to explore the heat and fluid flow mechanisms for two-sides and one-side heating (Cases A and B), based on the numerical results at $q^+w = 0.0043$, i.e. turbulent kinetic energy, temperature variance, turbulent heat flux, velocity and temperature profiles. Figure 6 illustrates the wall-normal distributions of the time-averaged flow velocity U/U_{max} at three different axial locations: x/H=0, 60, and 120. Figures 6(a) and (b) show the numerical results for Cases A and B respectively. The velocity U is normalized by the maximum value U_{max} at each axial location. The laminar flow profile is superimposed in the figure as a solid line, for comparison. In Figure 6(a) a substantial reduction of the velocity gradient takes place in the flow direction and the velocity profile approaches laminar one in the downstream region. In contrast, Figure 6(b) shows that the velocity gradients at the walls are slightly diminished along the flow, particularly in the vicinity of the heating wall, and the velocity profile is substantially different from the laminar one in the flow direction. The corresponding streamwise variations of the turbulent kinetic energy k for Cases A and B are illustrated in Figures 7(a) and (b) respectively. Here, the numerical results are normalized by a square of the wall friction velocity at the onset of heating u^{*2}. It is observed in Figure 7(a) that the turbulent kinetic energy level for two-sided heating (Case A) is extremely attenuated over the whole channel cross section in the flow direction due to high flux heating. This streamwise behavior is in accordance with that of the velocity distribution in Figure 6(a). The substantial attenuation in both velocity and turbulent kinetic energy is the same as the flow characteristics in the laminarizing flow in both the heated tube (Torii *et al.*, 1990; Torii and Yang; 1997) and the annuli heated from both inner and outer tube walls (Torii *et al.*, 1991). However, numerical results for Case B show that as the flow progresses, appreciable turbulent kinetic energy still remains in the velocity field, particularly near the insulated wall, as seen in Figure 7(b). This behavior corresponds to that of the velocity distribution in Figure 6(b) and is similar to that in the annular flow. That is, when the annular flow is strongly heated from one wall, the turbulent kinetic energy is severely diminished in the vicinity of the heating wall, while it is intensified near the opposite wall along the flow, as mentioned in the introduction. All these results consistently show that:

(1) if the flow is strongly heated from both side walls of the channel, laminarization occurs; and

(2) the trend towards laminarization from the strongly heated wall is always suppressed by the turbulent kinetic energy produced in the region near the insulated wall, where heat flux is added to the flow from one wall only.

Figures 8(a) and (b) show streamwise variations in the time-averaged temperature profile θ^+ for Cases A and B respectively. Numerical results are obtained at four different axial locations: x/H=0, 20, 60, and 120. Here, the radial profile at x/H=0 is uniform. Note that in Figure 8(a) only one-half of the channel cross section is represented because of the symmetry in the thermal field. The substantial reduction in the temperature gradient for Case A occurs

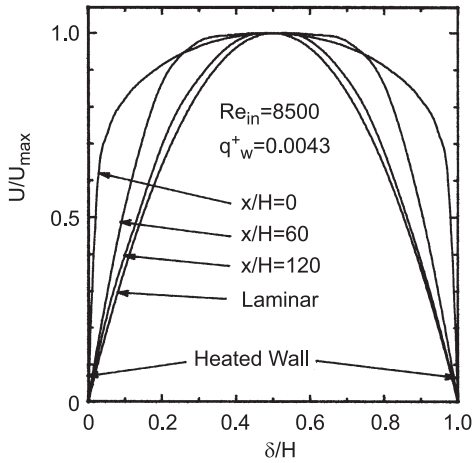

(a) two-sides heating

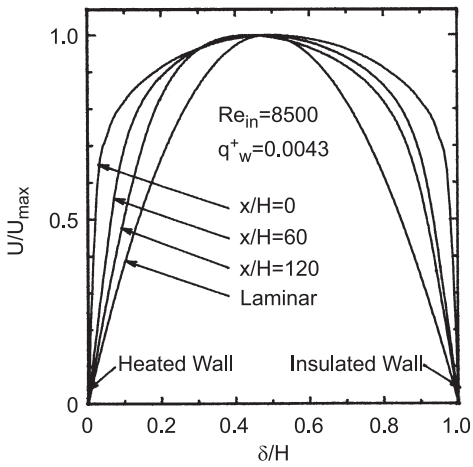

(b) one-side heating

Figure 6.
Variation of time-averaged streamwise velocity profiles in a strongly heated flow with three different axial locations

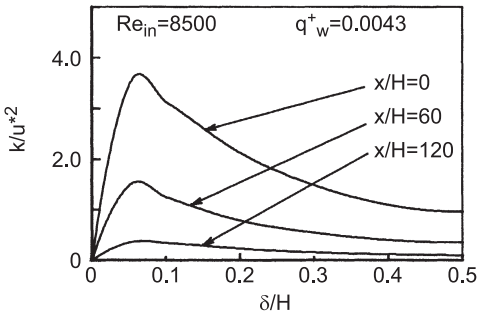

(a) two-sides heating

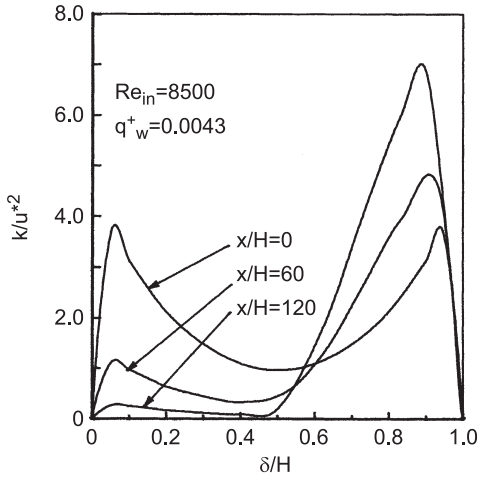

(b) one-side heating

Figure 7.
Variation of turbulent kinetic energy profiles in a strongly heated flow with three different axial locations

at the wall along the flow (Figure 8(a)), while numerical results of Case B reveal only a slight reduction in the temperature gradient at the heated wall in the flow direction (Figure 8(b)).

Figures 9(a) and (b) illustrate the radial distributions of the temperature variance $\overline{t^2}$ for Cases A and B respectively, in the thermal field. Numerical results are shown in each figure for different axial locations: x/H=0, 20, 60, and 120. Here, the temperature variance is divided by the square of the friction temperature t^* at each axial location. Notice that in Figure 9(a) only one-half of the channel cross section is represented as mentioned previously. As the flow moves in the downstream direction, there is a substantial reduction in $\overline{t^2}$ for Case A over the whole cross-section of the channel, as seen in Figure 9(a). This behavior implies an attenuation in the temperature fluctuations in the thermal field. For Case B, the predicted $\overline{t^2}$ at x/H=20 undergoes a sharp rise near the wall region followed by a gradual decline toward the other wall and as the flow moves along the channel, the temperature variance level $\overline{t^2}$ is somewhat

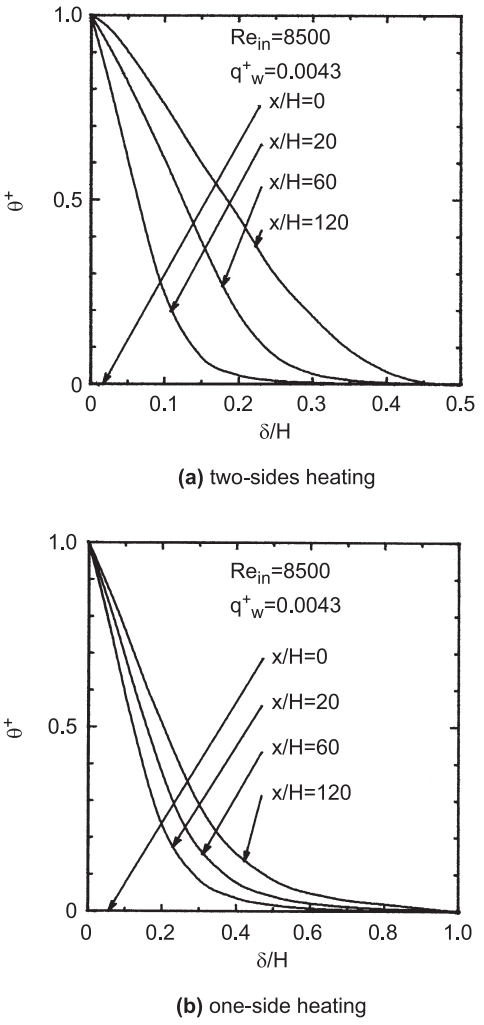

Figure 8.
Variation of time-averaged temperature profiles in a strongly heated flow with three different axial locations

diminished in the vicinity of the heated channel wall because of a decrease in the temperature gradient near that wall. In other words, appreciable temperature fluctuations remain in the thermal field when the flow is heated from one wall only.

Figures 10(a) and (b) illustrate the wall-normal turbulent heat flux profiles at different axial locations for Cases A and B respectively. For Case A, the wall-normal turbulent heat flux level in the vicinity of the wall is substantially reduced in the flow direction. This behavior is in accordance with the variation of the time-averaged temperature distribution, as seen in Figure 8(a). In contrast, the wall-normal turbulent heat flux level maintains to a certain degree along the flow. The corresponding distribution of the streamwise turbulent heat flux, $\overline{ut}$, was not depicted here, because $\overline{ut}$ exerts no direct effect on heat transfer.

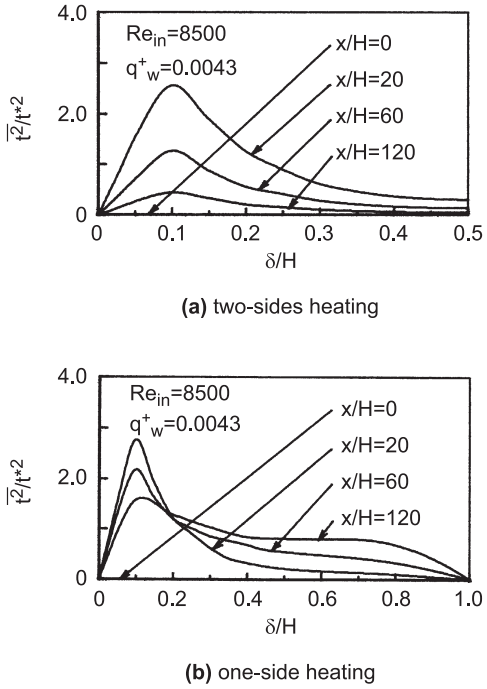

Figure 9.
Variation of temperature variance profiles in a strongly heated flow with three different axial locations

In summary, substantial reduction in the turbulent kinetic energy and temperature variance results in an attenuation in the Stanton number, as shown in Figure 5(a). One may thus conclude that a flow in a channel heated with uniform wall heat flux from both walls is laminarized, as are the tube and concentric annular flows. In contrast, a streamwise deterioration of the Stanton number in Figure 5(b) is suppressed by the presence of the turbulent kinetic energy produced in the vicinity of the insulated wall, even if the heat flux parameter satisfies the laminarization criterion for circular tube flows. That is, the trend towards laminarizing the flow is always suppressed if the heat flux is added to the flow from only one wall, even at levels that cause laminarization in a circular tube flow.

Next is to determine the criterion for the laminarization of flow in a two-dimensional channel heated under uniform wall heat flux from both side-walls. First of all, conditions should be specified under which the flow is certainly laminarized. Torii *et al.* (1990) established the criterion for the laminarizing flow in a tube with high heat flux using the k-ε turbulence model. That is, laminarization occurs when the calculated turbulent kinetic energy at the location 150 diameters downstream from the inlet becomes lower than one-tenth of the inlet value. The same idea, in which the criterion is for the turbulent kinetic energy at x/H=150 to be lower than one-tenth of its inlet value, is adopted in the present study. This is because the streamwise variation of a turbulent kinetic energy in the laminarizing flow, as depicted in Figure 7(a), is

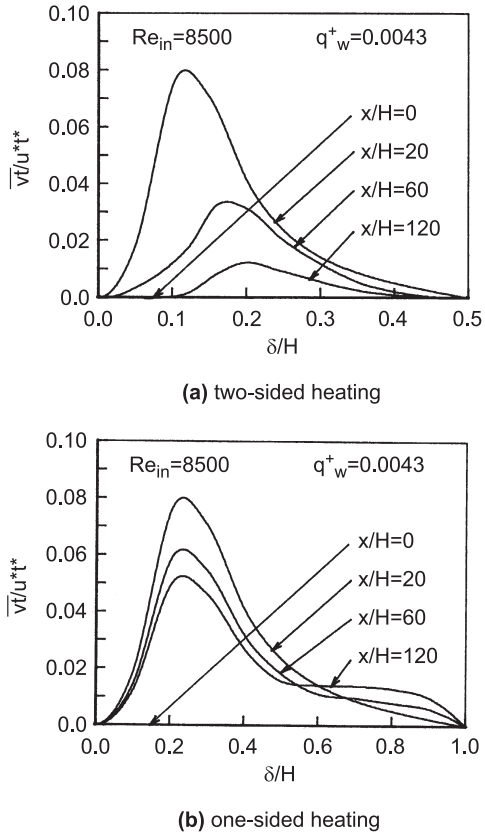

Figure 10.
Variation of wall-normal turbulent heat flux profiles in a strongly heated flow with three different axial locations

similar to that in the strongly heated tube case (Torii *et al.*, 1990). The predicted criterion is depicted in Figure 11, in which the existing criteria for the circular tube and the predicted criteria for the circular and annular tube flows (Torii *et al.*, 1990, 1991) are superimposed for comparison. It is observed that the criterion obtained here is similar to the circular and annular tube cases over a wide range of Reynolds numbers. One may thus conclude that a flow in a two-dimensional channel with uniform wall heat flux is laminarized at a same heating level as the circular and annular tube flow cases.

Summary

Anisotropic k-ε-$\bar{t^2}$-ε_t model has been employed to numerically investigate fluid flow and heat transfer in a channel heated with uniform heat flux. Consideration is given to the effects of passage geometry and boundary conditions on the occurrence of laminarization. The results are summarized as follows:

(1) If the channel is simultaneously heated from both walls with high uniform heat flux, a substantial reduction of the local Stanton number

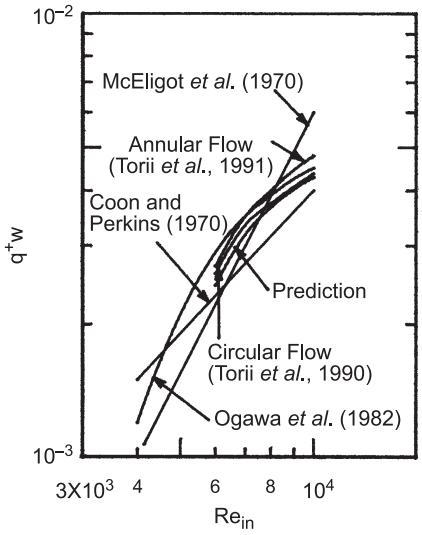

Figure 11.
A comparison of criteria for the occurrence of flow laminarization

causes laminarization along the flow. Therefore, the fluid flow in the channel is laminarized, just as in the circular and annular tube flow cases.

(2) When laminarization takes place, the velocity and temperature gradients in the vicinity of the channel wall decrease along the flow, resulting in a substantial attenuation in both the turbulent kinetic energy and the temperature variance over the entire channel cross section. Consequently, the turbulent heat flux is diminished by a decrease in the turbulent kinetic energy and temperature variance over the channel cross section, resulting in the deterioration of heat-transfer performance.

(3) If the channel is heated from only one side wall, substantial reduction of the local Stanton number is suppressed, resulting in no laminarization. This behavior is the same as that in an annulus heated with only one wall. This is because the trend towards laminarization is always suppressed by the turbulent kinetic energy produced in the region near the insulated wall.

(4) Criterion of laminarization in two-dimensional channel is similar to the circular and annular tube cases if the channel is strongly heated under the same heat flux level from both side-walls.

(5) If the laminarizing flow takes place, the occurrence of laminarization is affected by the boundary conditions of heating, while its effect of passage geometry is minor.

References

Abe, K., Kondoh, T. and Nagano, Y. (1994), "A new turbulence model for predicting fluid flow and heat transfer in separating and reattaching flows – I. flow field calculations", *Int. J. Heat Mass Transfer*, Vol. 37, pp. 139-51.

Bankston, C.A. (1970), "The transition from turbulent to laminar gas flow in a heated pipe", *Trans. ASME, Ser. C*, Vol. 92 No. 4, pp. 569-79.

Coon, C.W. and Perkins, H.C. (1970), "Transition from the turbulent to the laminar regime for internal convective flow with large property variations", *Trans. ASME, Ser. C*, Vol. 92 No. 3, pp. 506-12.

Ezato, K., Shehata, A.M., Kunugi, K. and McEligot, D.M. (1999), "Numerical prediction of transitional features of turbulent forced gas flows strong heating", *Trans. ASME, Journal of Heat Transfer*, Vol. 121 No. 8, pp. 546-55.

Fujii, S., Akino, N., Hishida, M., Kawamura, H. and Sanokawa, K. (1991), "Numerical studies on laminarization of heated turbulent gas flow in annular duct", *J. Atomic Energy Soc. Jpn.* (in Japanese), Vol. 33 No. 12, pp. 1180-90.

Kawamura, H. (1979), "Prediction of strongly heated turbulent flow of gas in a circular tube using a two-equation model of turbulence", *Trans. Jpn. Soc. Mech. Eng.* (in Japanese), Vol. 45 No. 395, B, pp. 1038-46.

Kays, W.M. and Crawford, M.E. (1980), *Convective Heat and Mass Transfer*, 2nd ed., MacGraw-Hill, New York, NY.

McEligot, D.M., Coon, C.M. and Perkins, H.C. (1970), "Relaminarization in tubes", *J. Heat & Mass Transf.*, Vol. 13 No. 2, pp. 431-3.

McEligot, D.M., Shehata, A.M. and Kunugi, T. (1998), "Prediction of strongly-heated internal gas flows", *Proc. 2nd International Conference in Turbulent Heat Transfer*, Vol. I, pp. 1-15.

Mori, Y. and Watanabe, K. (1979), "Reduction in heated transfer performance due to high heat flux", *Trans. Jpn. Soc. Mech. Eng.* (in Japanese), Vol. 45 No. 397, B, pp. 1343-53.

Myong, H.K. and Kasagi, N. (1990), "A new approach to the improvement of k-ε turbulence model for wall-bounded shear flows", *JSME Int. J., Ser. II*, Vol. 33 No. 1, pp. 63-72.

Nemira, M.A., Vilemas, J.A. and Simonis, V.M. (1980), "Heat transfer to turbulent flow of gases with variable physical properties in annuli (correlation of experimental results)", *Heat Transfer – Soviet Research*, Vol. 12, pp. 104-12.

Ogawa, M. and Kawamura, H. (1986), "Experimental and analytical studies on friction factor of heated gas flow in circular tube", *J. Atomic Energy Soc. Jpn.* (in Japanese), Vol. 28 No. 10, pp. 957-65.

Ogawa, M. and Kawamura, H. (1987), "Effects of entrance configuration on pressure loss and heat transfer of transitional gas flow in a circular tube", *Heat Transfer Japanese Research*, Vol. 15 No. 5, pp. 77-91.

Ogawa, M., Kawamura, H., Takizuka, T. and Akino, N. (1982), "Experimental study on laminarization of strongly heated gas flow in vertical circular tube", *J. Atomic Energy Soc. Jpn.* (in Japanese), Vol. 24 No. 1, pp. 60-7.

Patankar, S.V. (1980), *Numerical Heat Transfer and Fluid Flow*, Hemisphere, Washington, DC.

Perkins, K.R., Schade, K.W. and McEligot, D.M. (1973), "Heated laminarizing gas flow in a square duct", *J. Heat and Mass Transfer*, Vol. 16 No. 3, pp. 897-916.

Propath Group (1987), *Propath: A Program Package for Thermophysical Property*, Version 4.1.

Rodi, W. (1982), "Examples of turbulence models for incompressible flows", *AIAA, J.*, Vol. 20, pp. 872-9.

Schlighting, H. (1968), *Boundary-Layer Theory*, 6th ed., McGraw-Hill.

Shehata, A.M. (1984), "Mean turbulent structure in strongly heated air flows", PhD thesis, University of Arizona.

Torii, S. and Yang, W.-J. (1996), "A new near-wall two-equation model for turbulent heat transport", *Numerical Heat Transfer, Part A*, Vol. 29, pp. 417-40.

Torii, S. and Yang, W.-J. (1997), "Laminarization of turbulent gas flows inside a strongly heated tube", *Int. J. Heat Mass Transfer*, Vol. 40 No. 13, pp. 3105-18.

Torii, S., Shimizu, A. and Hasegawa, S. (1993), "Numerical analysis of laminarizing tube flows by means of a Reynolds stress turbulence model", *Heat Transfer-Japanese Research*, Vol. 22 No. 2, pp. 154-70.

Torii, S., Shimizu, A., Hasegawa, S. and Higasa, M. (1990), "Laminarization of strongly heated gas flows in a circular tube (numerical analysis by means of a modified k-ε model)", *JSME Int. J., Ser. II*, Vol. 33 No. 3, pp. 538-47.

Torii, S., Shimizu, A., Hasegawa, S. and Kusama, N. (1991), "Laminarization of strongly heated annular gas flows", *JSME Int. J., Ser. II*, Vol. 34 No. 2, pp. 157-68.